Flat Supercontinuum Generation From a Phosphorus-Doped Fiber

Kailong Li, Rui Song, Li Jiang, Zhiyong Pan, Zhiping Yan, and Jing Hou

***Abstract*—Phosphorus-doped fiber has great advantages in supercontinuum (SC) generation because it can narrow the gap between Raman-related peaks and valleys owing to its special Raman gain. In this paper, a random fiber laser (RFL) structure and a main oscillator power amplifier (MOPA) structure are used to pump a self-made phosphorus-doped fiber. The results show that the output spectrum of the latter structure is more favorable in spectral flatness improvement. The 15 dB bandwidth covers from 690 nm to 2320 nm and the output power is 15.1 W. In the range of 1076 -2010 nm, the spectral intensity fluctuates within 3 dB. To the best of our knowledge, the spectral range and flatness are the best among SC generation based on phosphorus-doped fiber methods, which provide a solution for improving the spectral characteristics of the SC**

***Index Terms*—Fiber amplifier, flat supercontinuum, nonlinear optics, phosphorus-doped fiber.**

I. Introduction

THE supercontinuum (SC) has the characteristics of wide spectrum, high brightness, and high spatial coherence, which plays an important role in the fields of hyperspectral lidar, photoelectric countermeasures and optical coherence tomography [1], [2], [3], [4], [5]. Its generation mainly involves a high peak power pumping source and a nonlinear medium, which usually using an ultra-short pulse laser to pump a piece of photonic crystal fiber (PCF) [6], [7], [8]. The spectrum can greatly broadened under the comprehensive influence of a variety of nonlinear effects and dielectric dispersion [9], [10], [11].

At present, the main schemes for SC generation in near infrared band mainly including nonlinear fiber amplifier directly generating SC method, a fiber laser to pump a piece of PCF method, and using a random fiber laser (RFL) structure to generate SC method [7], [12], [13]. SC generation from a nonlinear fiber amplifier method has a high conversion efficiency and can achieve high power output, but its threshold of SC generation is relatively high and the output spectrum flatness is relatively poor. A fiber laser using single-stage or multistage amplifier to pump PCF to generate SC method has wide spectrum width and high spectral flatness owing to the flexible dispersion design and high nonlinearity of PCF; but its structure is usually complex and the cost is high. In order to achieve effective strengthening of the short-wave portion of SC, the core size of the PCF is often designed to be extremely small, which makes it difficult to withstand the high power and there is a mode mismatch between it and the pigtail of the pumped fiber laser. The RFL structure to generate SC method use the random distributed feedback provided by Rayleigh scattering in the fiber as the cavity mirror and use stimulated Raman scattering or Brillouin scattering as the gain [14]. When the gain is larger than the loss, the laser and SC can be generated [15]. This method is simple in structure and can greatly reduce the cost of SC, and it is currently in a stage of rapid development.

Our group has carried out a series of studies on the above three SC generation schemes. In terms of SC generation from fiber amplifier method, a 714 W SC is achieved in a four-stage MOPA configuration with a spectral range of 690-2350 nm [12]. By adding a piece of passive fiber in the last stage ytterbium-doped fiber amplifier, the 10 dB width can cover 1050-2095 nm, which greatly improved the spectral flatness and width of this method. In addition, by using graded-index multimode fiber the output SC spectrum can cover 580-2400 nm [16]. In terms of SC generation with PCF, a 80 W SC with spectrum covers 350-2400 nm is achieved in a seven core PCF [7]. The pump is a self-made high power 1016 nm mode locked fiber laser and the zero-dispersion-wavelength (ZDW) of the PCF is around 991 nm. In terms of SC generation using a RFL structure, the first visible to near-infrared SC directly from a RFL, the first SC generation directly from a RFL based on PCF, based on polarization-maintaining fiber, with ultr-compact and ultra-short cavity have been achieved by our group [17], [18], [19], [20].

Nonlinear fiber medium is a key factor in SC generation. The generation of SC is closely related to nonlinear effects such as soliton splitting, stimulated Raman scattering, four-wave mixing, self-phase modulation and cross-phase modulation [9], [10], [11]. The stimulated Raman scattering affects the extension of the SC to the long-wave direction in the normal dispersion region. In the ordinary silica fiber, the effective Raman conversion only occurs in the typical frequency shift range of about 13.2 THz. Therefore, in the reported output spectrum of SC source based on solid silica fiber, there are periodic Raman-related peaks and valleys in the normal dispersion region of the fiber, which greatly deteriorate the spectral flatness [12], [17]. In 2024, Zhang proposed that phosphorus-doped fiber (PDF)

Received 16 October 2024; revised 15 November 2024; accepted 16 November 2024. Date of publication 21 November 2024; date of current version 2 December 2024. This work was supported by the Natural Science Foundation of Hunan Province under Grant 2022JJ30653. *(Corresponding authors: Rui Song; Jing Hou.)*

The authors are with the College of Advanced Interdisciplinary Studies, National University of Defense Technology, Changsha 410073, China, also with the Nanhu Laser Laboratory, National University of Defense Technology, Changsha 410073, China, and also with the Hunan Provincial Key Laboratory of High Energy Laser Technology, National University of Defense Technology, Changsha 410073, China (e-mail: srnotice@163.com; houjing25@sina.com).

Digital Object Identifier 10.1109/JPHOT.2024.3504277

has a wider and flatter Raman gain spectrum than germanium-doped fiber (GDF), and replacing germanium-doped fiber with phosphorus-doped fiber is conducive to improving the spectral flatness of the output SC [21]. PDF shows great potential to generate flat SC as a new nonlinear fiber medium. Zhang used a 1064 nm pulsed laser with a maximum average power of 841 mW to pump 500 m PDF with a core/cladding diameters of 5/125 μm, and achieved a flat SC spanning from 850 nm to 2150 nm, which proved the advantages of PDF compared with GDF. Prior to this, there have been reports of using PDF to generate SC by the cascade Raman effect [22]. However, it does not clearly demonstrate the advantages of doping phosphorus elements, and the power level is below watts level, and the spectral range is about 500 nm. Schemes for generating SC spectra using phosphate-doped PCF have also been reported. D. Labat et al. obtained an average output power of 36 W and a spectral coverage of 570 nm-1700 nm using a phosphorus-doped PCF with a ZDF of about 1 μm [23]. This scheme enhances the spectral power density of the short-wave by controlling the group velocity dispersion (GVD) of PCF, but spectral expansion above 1700 nm is limited by the significant enhancement of optical soliton attenuation in the range of 1600 nm-1700 nm. The subsequent power increase of this scheme is limited by the thermal management problem of PCF.

In our work, in order to increase the output power of SC and further improve the output spectral characters, two batches of PDF are designed and produced. We select a batch of PDF with stronger nonlinear coefficients to carry out follow-up experiments. In addition, a MOPA structure and a RFL structure are designed and compared to pump the PDF to generate SC. It is found that the MOPA structure scheme has advantages in pump power conversion and spectral flatness improvement. Finally, we amplified a 1064 nm seed to 32.1 W in a two-stage MOPA structure and then to pump 30 m PDF. A flat SC with a power of 15.1 W and a spectrum ranging from 685-2350 nm is obtained. This SC source exhibits a flat spectrum ranging from 690 nm to 2320 nm at a 15 dB level and in the range of 1076-2010 nm, the spectral intensity fluctuates within 3 dB, which shows the great potential of the PDF in flat SC generation.

II. Experimental Setup

In order to analyze the effect of the cavity structure on SC generation based on PDF, a RFL structure and a two-stage MOPA structure are designed and the experimental setup are shown in Fig. 1.

The RFL structure with a single-stage half-open cavity is shown in Fig. 1(a), wherethe optical fiber mirror (OFM) with 40 nm bandwidth and 1064 nm central wavelength is utilized at one end of the cavity to provide broadband feedback. These two 976 nm pump laser diodes (LD) have a maximum pump power of 22.4 W and 24.4 W respectively, and these pump are injected into a 5 m 10/130 μm Ytterbium-doped double clad fiber (YDF) through a $(2 + 1) \times 1$ fiber combiner. Then a piece of self-made 10/130 μm PDF is followed the YDF, and the output end of the PDF is cleaved at an angle of 8°to avoid end feedback. Fig. 1(b) shows the MOPA structure, which uses a 1064 nm

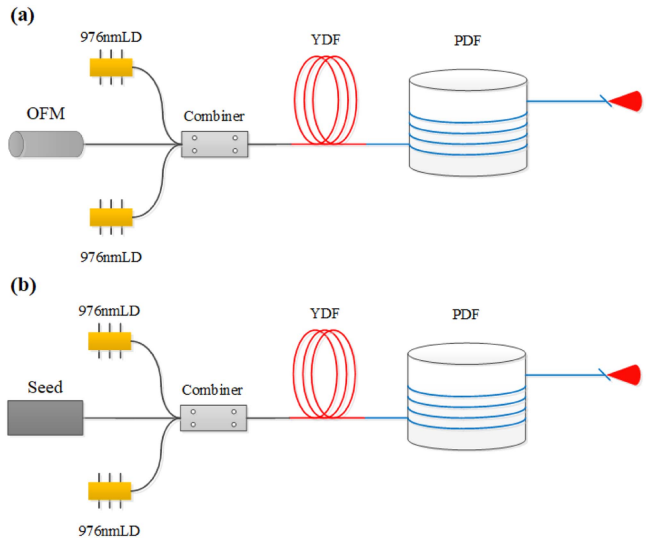

Fig. 1. The experimental setup for flat SC generation: (a) RFL structure and (b) MOPA structure.

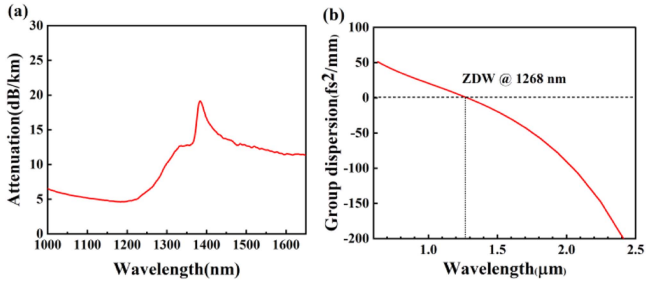

Fig. 2. The loss curve and the dispersion curve of PDF.

pulsed fiber laser (Connet, VLSS-1064-B-200-FA) as the seed with adjustable repetition rate and pulse width and its maximum average output power is 800 mW. A fiber amplifier is followed by the seed, these two 976 nm LDs, the YDF, and the fiber combiner keep the same as that in Fig. 1(a). The PDF output end is also cleaved at an angle of 8°to prevent end feedback.

The PDF used in the experiment is a self-made double-clad fiber with a core/cladding diameters of 10/130 μm. The core NA is 0.1 and the phosphorus doping concentration is around 6 mol%. As shown in Fig. 2(a), the loss curve of PDF is measured by a fiber analysis system (Photon Kinetics, PK2300). We use the fiber analysis system to measure 500 m PDF based on optical time-domain reflectometer (OTDR) in PK2300. The COMSOL MULTIPHYSICS software as well as the MATLAB software are used during the calculation. First, the geometric value (the radius of the core and the cladding) and the refractive index of the core and the cladding are used to build a simulation model of PDF in the COMSOL MULTIPHYSICS software. Next, this model is used to calculate the distribution of the electromagnetic field in the fiber. Then, the model is transformed into a .m type file, which will be used in the following calculation in the MATLAB software. In MATLAB, algorithm we programmed calls the model to estimate the effective refractive index (n_{eff})

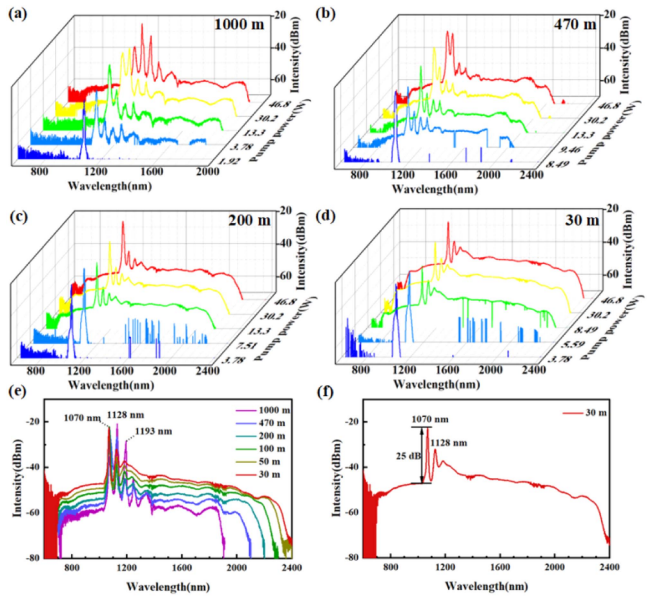

Fig. 3. Spectral evolution with increasing pump power under different PDF lengths: (a) 1000 m, (b) 470 m, (c) 200 m, and (d) 30 m. (e) The output spectra vary with the PDF length under maximum pump power. (f) The output spectrum of 30 m PDF under maximum pump power.

in the wavelength ranging from 600 nm to 2500 nm based on the Sellmeier equation. In the last step, the matrix of the n_{eff} is used to get the parameter of β_1 through the polynomial fit. The dispersion curve of the fundamental mode in PDF can be obtained using the expressions: $D = \mathrm{d}\beta_1/\mathrm{d}\lambda$ where D represents the dispersion parameter. The calculation results are shown in Fig. 2(b).

III. Experimental Results and Discussion

The output spectrum of the SC is collected by two optical spectrum analyzers (Yokogawa, AQ6374 and AQ6375) with spectral bands of 350-1750 nm and 1200-2400 nm respectively. The measured spectra are spliced together by aligning the spectral intensity at 1500 nm.

A. SC Generation in RFL Structure

In the process of SC generation, the length of the nonlinear fiber medium is an important factor. In the experiment, six sets of PDFs with different lengths of 30 m, 50 m, 100 m, 200 m, 470 m, and 1000 m are used to conduct the output spectrum comparison experiment under the maximum pump power. The experimental results are shown in Fig. 3. In the RFL structure, the nonlinear fiber not only plays the role for nonlinear broadening, but also acts as the cavity mirror through the random distributed feedback provided by the reverse Rayleigh scattering in the fiber [14], [15]. First, as shown in Fig. 3(a)–(d), substantial random spectral spikes with various bandwidth can be observed over the blue line in the spectrum (especially in Fig. 3(c) and (d)), which are caused by the interaction between Rayleigh scattering and stimulated Brillouin scattering effects [14]. Further increasing the pump power, a series of intensity peak appear in the spectrum and the corresponding wavelengths correspond to 1128 nm and 1193 nm. The corresponding frequency shift of each intensity peak to adjacent peak is about 14.5 THz, meaning the stimulated Raman scattering effect dominates the initial spectral broadening, which consists with the initial spectral evolution of the pump in the normal dispersion region. Subsequently, a wide band SC is formed by the combination of four wave mixing, soliton effect and other nonlinear effects. Notably, when the fiber length reaches 1000 m, the cascade Raman peaks are clearly shown in Fig. 3(a). This is because the lower threshold of the Raman effects and the stronger random distributed feedback brought by the longer fiber length result in the enhanced intensity of Raman peaks.

We compared the output spectra of six groups of PDF lengths under the same pump power, as shown in Fig. 3(e). It can be seen that the long-wavelength boundary of the output spectrum continues to shorten with the increase of the PDF length. This is because the longer length of the fiber, the transmission loss is higher, especially in the long-wavelength region with the high fiber loss. Therefore, the shorter fiber can effectively reduce the transmission loss and avoid long-wave boundary shrinkage. However, when the fiber length is reduced to about 50 m, the impact of further shortening the fiber length is no longer obvious. At the same time, considering that the random fiber laser requires a certain length of fiber to provide distributed feedback, the fiber length is not further reduced after the fiber is shortened to 30 m. The random distributed feedback in the fiber is relatively weak, and the pump light at 1070 nm has not undergone sufficient nonlinear effect conversion. As shown in Fig. 3(f), there is a strong pump residual peak (25 dB) in the output spectrum, which concentrates most of the pump light energy.

B. SC Generation in MOPA Structure

For the two-stage MOPA structure used in Fig. 1(b), one of the key parameters that can be adjusted in the cavity is the time domain parameter of the pulsed seed laser, and the other is the length of the PDF. When the average output power of the pulsed seed laser is certain, a smaller pulse repetition rate means a higher peak power of the laser, and results in a stronger nonlinear effects in the process of transmission. A stronger nonlinear effects is conducive to the broadening of the laser spectrum. If the peak power of the seed pulse is too high, the laser spectrum will expand earlier in the YDF, which is not conducive for power scaling. So it is necessary to find a suitable pulse repetition rate to balance pump laser power scaling and subsequent spectral broadening [12].

The maximum average output power of the seed is 800 mW, and the pulse repetition rate is adjustable from 100 kHz to 3 MHz. First, the output spectra of the amplifier at different seed pulse repetition rates are tested. As shown in Fig. 4(a), when the pulse repetition rate is 500 kHz, the higher peak power causes the laser spectrum to expand prematurely in the YDF, affecting the amplifier efficiency. When the pulse repetition rate increases to 1.2 MHz and 2.2 MHz in Fig. 4(b) and (c), the peak laser power begins to decrease, and the spectral broadening in YDF is suppressed. As shown in Fig. 4(c) and (d), when the pulse

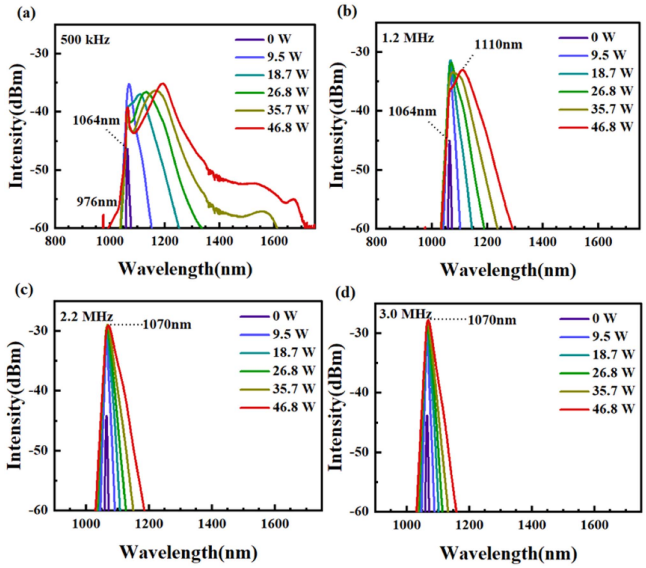

Fig. 4. The output spectra of the amplifier at different pulse repetition rates: (a) 500 kHz, (b) 1.2 MHz, (c) 2.2 MHz and (d) 3 MHz.

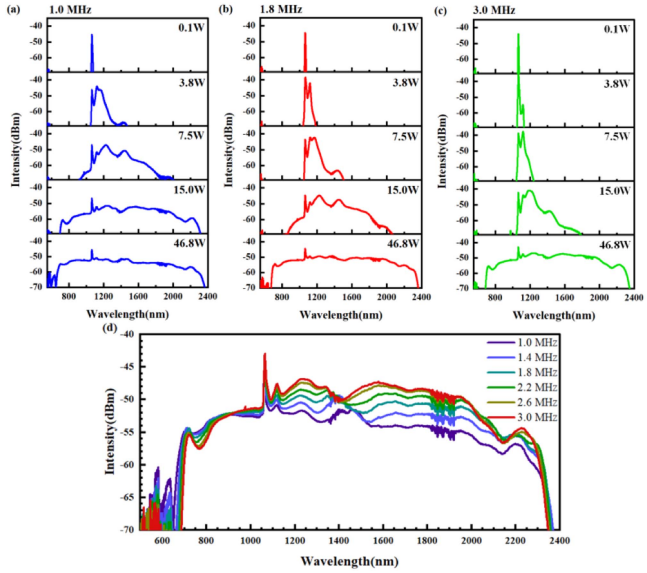

Fig. 5. The output spectrum evolves with the increase of pump power when the pulse repetition rate is (a) 1.0 MHz, (b) 1.8 MHz and (c) 3.0 MHz. (d) The output spectrum changes with the increase of the pulse repetition rate.

TABLE I
THE OUTPUT POWER VARIES WITH THE SEED PULSE REPETITION RATE

Seed pulse repetition rate(MHz)	Output power (W)
1.0	8.0
1.4	10.5
1.8	13.0
2.2	15.1
2.6	17.0
3.0	17.7

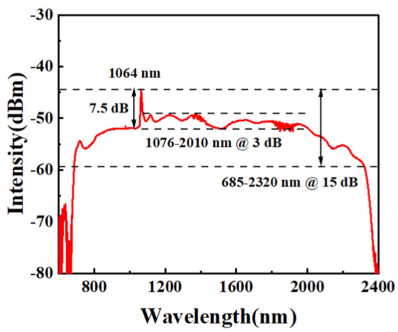

Fig. 6. PDF-based SC pumped by MOPA structure at the seed repetition rate of 2.2 MHz.

repetition rate is in the range of 2.2 MHz to 3 MHz, the output spectrum and power after the amplifier are similar.

After the amplifier, the amplified laser is injected into 30 m PDF for SC generation. In the range of 1 MHz to 3 MHz, a series of seed pulse repetition rates are selected for control experiments and the experimental results are shown in Table I and Fig. 5. When the repetition rate increases from 1 MHz to 3 MHz, the output power after the amplifier increases from 30.3 W to 32.2 W, and the output power after PDF increases from 8.03 W to 17.7 W, as shown in Table I. When the laser peak power is higher, the nonlinear effect is stronger, the quantum loss caused by the frequency conversion is higher, and the light with a wavelength larger than 2400 nm is disappeared in the form of heat energy due to the huge transmission loss of PDF in the long-wave. When the repetition rate increases, the energy loss caused by quantum loss and long-wavelength loss decreases, so the output power increases significantly.

By comparing Fig. 5(a) and (b), it is found that the lower the pulse repetition rate, the lower the threshold power of SC generation, which is due to the stronger nonlinear effect caused by the higher peak power. From Fig. 5(d), when the repetition frequency gradually increases from 1 MHz to 3 MHz, the short-wave boundary of the spectrum tends to shrink and the spectral intensity decreases in the 600 nm to 900 nm range due to the weakening of nonlinear effects. In the 1100 nm to 2000 nm range, laser with a lower repetition frequency has a higher peak power, causing the energy in this spectrum transferred to longer wavelengths. However, due to the large loss of PDF above 2 μm, the light undergoing the frequency conversion is lost and cannot be reflected in the output spectrum. Therefore, appropriately increasing the pulse repetition rate can enhance the spectral intensity from 1100 nm to 2000 nm and improve the output power. However, when the laser peak power is too low, the weak nonlinear effect leads to insufficient spectrum broadening and the overall flatness of the spectrum decreases. According to the above considerations, when the seed pulse repetition rate is 2.2 MHz, high output power, high energy conversion efficiency and better spectral flatness can be achieved.

When the seed pulse repetition rate is 2.2 MHz, As shown in Fig. 6, the intensity of the pump residual peak in the spectrum is 7.5 dB, which is much lower than the 25 dB pump residual

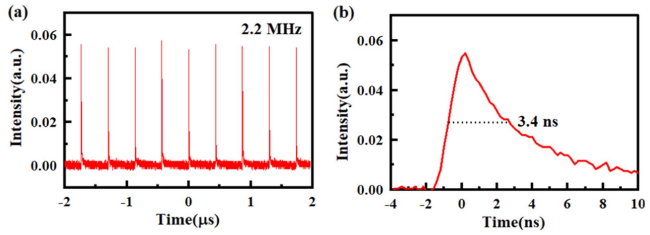

Fig. 7. The time domain information of the amplified laser.

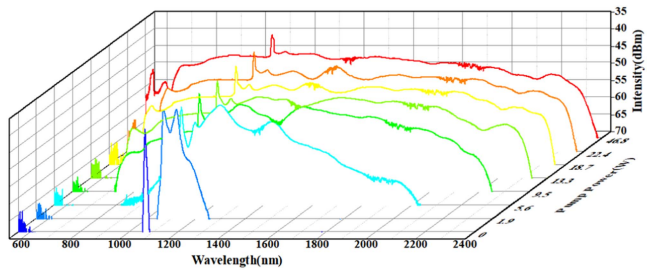

Fig. 8. Spectral evolution with increasing pump power at the seed repetition rate of 2.2 MHz.

peak in the previous scheme, indicating that the MOPA structure has a higher pump energy conversion efficiency than the RFL structure.

C. Flat SC Generation With PDF in a MOPA Structure

In the above two sections, SC is generated by pumping a piece of PDF with RFL structure and MOPA structure respectively and the MOPA structure has more advantages in pump power conversion efficiency and spectral flatness. In this section, we will analyze how to optimize the parameters of the MOPA structure to pump PDF to generate SC with optimal spectral characters. In this section, the process of generating flat SC in scheme 2 is discussed in detail.

The experimental structure is shown in Fig. 1(b). The average pumping power of the seed is 800 mW, the pulse repetition rate is set at 2.2 MHz, and the pulse width is set at 1 ns. After a fiber amplifier with a total pumping power of 46.8 W, the laser output power is amplified to 32.1 W, in which the conversion efficiency of the 976 nm pump light to the 1 μm laser light is 68.6%. The output spectrum of the amplifier is shown in Fig. 4(b) and time domain information is shown in Fig. 7. Then the amplified laser is injected into a 30 m PDF to obtain SC. The evolution of the spectrum with the increase of the pump power of the amplifier is shown in Fig. 8.

When the pump power of the amplifier is 0 W, the output spectrum at 1064 nm is symmetrically broadened under self-phase modulation [9]. With the increase of the pump power, Raman related peaks gradually appear in the spectrum, and the spectrum continues to expand to the long-wave direction under cascade stimulated Raman scattering effect. When the long-wave edge of the spectrum is widened above the ZDW of PDF, modulation instability (MI) begins to work and the energy of the high frequency light is continuously pumped to

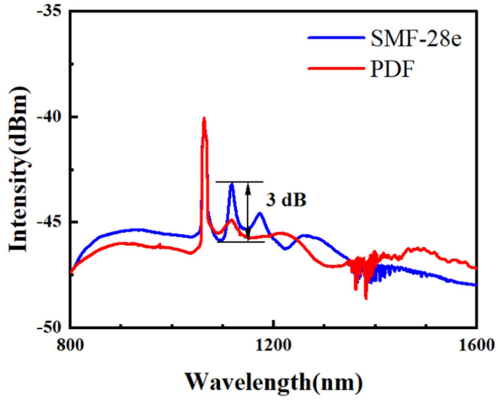

Fig. 9. The MOPA structure pumps PDF and SMF-28e respectively to generate SC.

the low frequency light under the combined action of soliton fission, soliton self-frequency shift and the spectrum continues to expand in the direction of long-wave region [24]. The dispersion curve of PDF is shown in Fig. 2(b). At the same time, the soliton pulse will be subjected to high-order dispersion perturbations during transmission, which will make the soliton pulse unstable and emit dispersive waves (DW) to the short-wave region through Cherenkov radiation [25]. The frequency of DW is determined by the phase matching condition, which requires the phase velocity of DW to match the soliton pulse. Finally, under the maximum LD pump power of 46.8 W, the signal light is amplified to 32.1 W, and the generated SC has a power of 15.1 W after PDF. The spectrum ranges from 685-2350 nm, compared with the reported PDF-based SC scheme, the spectrum is further expanded by about 300 nm and the power has been increased from mW to 10 W level. In the range of 1076-2010 nm, the spectral intensity fluctuates within 3 dB and the Raman-related peaks and valleys are suppressed within 2 dB.

In order to verify the advantages and potential of PDF in generating flat SC schemes, a 30 m SMF-28e (Corning) is used to replace PDF in Fig. 1(b) under the same conditions. The comparison results are shown in Fig. 9. SME-28e is a germanium-doped fiber with ultra-low absorption and good performance in SC generation, and it has a core/cladding diameters of 8/125 μm. From the spectral comparison in Fig. 9, the spectrum generated from PDF has a better spectral flatness in the Raman gain region, while the spectrum generated from SMF-28e has a first-order Raman peak with an intensity of about 3 dB. We use the spectral integration method to calculate the power of the first-order Raman (1096 nm-1146 nm) peaks of the two spectra as 1.26 W (SMF-28e) and 0.80 W (PDF), respectively. It is proved that PDF has advantage and great potential in SC spectral flatness improvement.

IV. Conclusion

In summary, a PDF with large core size and optimal doping concentration is designed and drawn by our own fiber drawing tower, and a RFL structure and a MOPA structure are constructed to carried out SC generation comparison experiments. The parameters that affect the SC output characters have been analyzed

in detail which including the length of the PDF, the repetition rate of the laser seed, the structure of the laser cavity. The results show that the MOPA structure is more suitable for flat SC generation. The amplified pump laser with a power of 32.1 W is injected into the PDF, resulting in a flat SC with a power of 15.1 W and a spectrum ranging from 685 nm to 2350 nm. The source exhibits a flat spectrum ranging from 690 nm to 2320 nm at a 15 dB level. In the range of 1076-2010 nm, the spectral intensity fluctuates within 3 dB and the Raman-related peaks and valleys are suppressed within 2 dB. Compared with the reported PDF-based SC generation scheme, the spectral coverage is extended by about 300 nm and the output laser power is improved by more than two order of magnitude. This paper provides an easy and cost-effective method to improve the spectral characters of the SC. In addition, the output power and the spectral flatness can be further improved by adding amplifiers in the MOPA structure, which will be carried out in our future work.

ACKNOWLEDGMENT

The authors are grateful to Sen Guo for his helping during the experiment.

REFERENCES

[1] R. R. Alfano, *The Supercontinuum Laser Source: The Ultimate White Light*. Berlin, Germany: Springer, 2016.

[2] A. Manninen, T. Kääriäinen, T. Parviainen, S. Buchter, M. Heiliö, and T. Laurila, "Long distance active hyperspectral sensing using high-power near-infrared supercontinuum light source," *Opt. Exp.*, vol. 22, pp. 7172–7177, 2014.

[3] M. K. Dasa et al., "All-fibre supercontinuum laser for in vivo multispectral photoacoustic microscopy of lipids in the extended near-infrared region," *Photoacoustics*, vol. 18, 2020, Art. no. 100163.

[4] M. Yamanaka, H. Kawagoe, and N. Nishizawa, "High-power supercontinuum generation using high-repetition-rate ultrashort-pulse fiber laser for ultrahigh-resolution optical coherence tomography in 1600 nm spectral band," *Appl. Phys. Exp.*, vol. 9, 2016, Art. no. 022701.

[5] J. Barrick, A. Doblas, M. R. Gardner, P. R. Sears, L. E. Ostrowski, and A. L. Oldenburg, "High-speed and high-sensitivity parallel spectral-domain optical coherence tomography using a supercontinuum light source," *Opt. Lett.*, vol. 41, pp. 5620–5623, 2016.

[6] J. M. Dudley and J. R. Taylor, "Ten years of nonlinear optics in photonic crystal fibre," *Nat. Photon.*, vol. 3, pp. 85–90, 2009.

[7] X. Qi et al., "High-power visible-enhanced all-fiber supercontinuum generation in a seven-core photonic crystal fiber pumped at 1016 nm," *Opt. Lett.*, vol. 43, pp. 1019–1022, 2018.

[8] H. Zhang et al., "All-fiber high power supercontinuum generation by cascaded photonic crystal fibers ranging from 370 nm to 2400 nm," *IEEE Photon. J.*, vol. 12, no. 2, Apr. 2020, Art. no. 7101608.

[9] J. M. Dudley and J. R. Taylor, *Supercontinuum Generation in Optical Fibers*. Cambridge, MA, USA: Cambridge Univ. Press, 2010.

[10] X. Xie, Y. Deng, and S. L. Johnson, "Compact and robust supercontinuum generation and post-compression using multiple thin plates," *High Power Laser Sci. Eng.*, vol. 9, 2021, Art. no. e66.

[11] J. Li et al., "Research progress of high-power visible to near-infrared supercontinuum source," *Acta Optica Sinica*, vol. 43, 2023, Art. no. 26256.

[12] L. Jiang, R. Song, J. He, and J. Hou, "714 W all-fiber supercontinuum generation from an ytterbium-doped fiber amplifier," *Opt. Laser Technol.*, vol. 161, 2023, Art. no. 109168.

[13] L. Jiang et al., "Kilowatt-level supercontinuum generation in a single-stage random fiber laser with a half-open cavity," *High Power Laser Sci. Eng.*, vol. 11, 2023, Art. no. e80.

[14] D. V. Churkin et al., "Recent advances in fundamentals and applications of random fiber lasers," *Adv. Opt. Photon.*, vol. 7, pp. 516–569, 2015.

[15] R. Ma, W. L. Zhang, S. S. Wang, X. Zeng, H. Wu, and Y. J. Rao, "Simultaneous generation of random lasing and supercontinuum in a completely-opened fiber structure," *Laser Phys. Lett.*, vol. 15, 2018, Art. no. 085111.

[16] L. Jiang, R. Song, and J. Hou, "Hundred-watt level all-fiber visible supercontinuum generation from a graded-index multimode fiber," *Chin. Opt. Lett.*, vol. 21, 2023, Art. no. 051403.

[17] L. Chen, R. Song, C. Lei, W. Yang, and J. Hou, "Random fiber laser directly generates visible to near-infrared supercontinuum," *Opt. Exp.*, vol. 27, pp. 27308–27315, 2019.

[18] J. He, R. Song, Y. Tao, and J. Hou, "Supercontinuum generation directly from a random fiber laser based on photonic crystal fiber," *Opt. Exp.*, vol. 28, pp. 27308–27315, 2020.

[19] J. He, R. Song, L. Jiang, W. Yang, and J. Hou, "Supercontinuum generated in an all-polarization-maintaining random fiber laser structure," *Opt. Exp.*, vol. 29, pp. 28843–28851, 2021.

[20] J. He, R. Song, W. Yang, and J. Hou, "A near-infrared supercontinuum light source with ultra-short cavity structure," *Chin. J. Lasers*, vol. 48, pp. 19140–19146, 2021.

[21] Y. Zhang et al., "Phosphorus-doped fiber for flat octave spanning supercontinuum generation," *Opt. Lett.*, vol. 49, pp. 830–833, 2024.

[22] S. Kobtsev, S. Kukarin, S. Smirnov, and I. Ankudinov, "Cascaded SRS of single- and double-scale fiber laser pulses in long extra-cavity fiber," *Opt. Exp.*, vol. 22, pp. 20770–20775, 2014.

[23] D. Labat et al., "Phosphorus -doped photonic crystal fibers for high-power (36 W) visible CW supercontinuum," *IEEE Photon. J.*, vol. 3, no. 5, pp. 815–820, Oct. 2011.

[24] J. C. Travers, A. B. Rulkov, B. A. Cumberland, S. V. Popov, and J. R. Taylor, "Visible supercontinuum generation in photonic crystal fibers with a 400 W continuous wave fiber laser," *Opt. Exp.*, vol. 16, pp. 14435–14447, 2008.

[25] F. Biancalana, D. V. Skryabin, and A. V. Yulin, "Theory of the soliton self-frequency shift compensation by the resonant radiation in photonic crystal fibers," *Phys. Rev., E*, vol. 70, 2004, Art. no. 016615.